

## Research Article

# Harmonic Analysis of Precipitation Time Series in Lake Tana Basin, Ethiopia

Zewdu Alamineh Fetene <sup>1,2</sup>, Tesfay Mekonnen Weldegerima <sup>1</sup>, Tadesse Terefe Zeleke,<sup>3</sup> and Melessew Nigusie<sup>4</sup>

<sup>1</sup>Atmospheric Physics, Bahir Dar University, P.O. Box 79, Bahir Dar, Ethiopia

<sup>2</sup>Physics Department, Debretabor University, Debre Tabor, Ethiopia

<sup>3</sup>Institute of Geophysics, Space Science and Astronomy, Addis Ababa University, Addis Ababa, Ethiopia

<sup>4</sup>Washer and Radar Science Research Laboratory, Bahir Dar University, Bahir Dar, Ethiopia

Correspondence should be addressed to Zewdu Alamineh Fetene; [alamineh.zewdu36@gmail.com](mailto:alamineh.zewdu36@gmail.com)

Received 20 December 2017; Revised 15 March 2018; Accepted 3 April 2018; Published 7 June 2018

Academic Editor: Efthymios I. Nikolopoulos

Copyright © 2018 Zewdu Alamineh Fetene et al. This is an open access article distributed under the Creative Commons Attribution License, which permits unrestricted use, distribution, and reproduction in any medium, provided the original work is properly cited.

This study presents harmonic analysis of precipitation observations within the Lake Tana Basin for the periods of 1985–2015. The livelihood of several millions of people within the basin and outside the basin is governed by the precipitation conditions within this basin. Large spatial and temporal variabilities of precipitation can increase the incidence of extreme events such as floods and droughts. It is important to identify the characteristics of these variations, and this study aims at investigating the characteristics of the seasonal and annual cycles of precipitation within the Lake Tana Basin using harmonic analysis. Precipitation data of 31 years from four weather stations were used in the analysis. We then applied harmonic analysis to calculate the amplitude, phase shift, and variance of observation. Detailed characteristics of the first five harmonics are presented and discussed. We found the amplitude of the first harmonic to be 173.42, 177.93, 127.77, and 188.78 mm for Debre Tabor, Bahir Dar, Gondar, and Dangila, respectively. This shows that Dangila areas got more rainfall during this fundamental period than others increasing from Gondar to Dangila direction. Also, the variance in the first harmonic is smaller than the variances of other harmonics, and this means that the large variations of the precipitation originate from higher harmonics (short time periods). This shows that precipitation variations are governed mainly by monthly, seasonal, and semiannual variations. The analysis has shown that maximum precipitation for all stations occurred in July and August.

## 1. Introduction

The impacts of climate change and climate variability on human life are widely acknowledged. These led to monitor the behavior of weather and climate variables. Rainfall, as one of the most important climate variables, has a direct and indirect impact on the natural environment and human life. Large spatial and temporal variability of it leads to increased incidence of extreme events such as droughts and floods [1]. Drought has three distinguishing features that depend on the characteristics of precipitation; such as intensity, duration and spatial coverage [2]. Floods include river floods, flash floods, urban floods, and sewer floods and can be caused by intense and/or long-lasting precipitation, dam break, and reduced conveyance due to landslides.

Many studies have shown the spatial and temporal changes in the amount, intensity, and duration of rainfall worldwide. For example, a study of rainstorms in China [3] has shown an increase in rainfall in the subtropical areas. Rainfall shows a decreasing trend in Inner Mongolia [4] from 1960 to 2012. Similarly, a study on long-term trend in precipitation of different spatial regions of Bangladesh [5] suggested that, for annual precipitation, a significant increasing monotonic trend was found in whole Bangladesh.

One of the advanced techniques of studying the rainfall distributions and variabilities is the harmonic analysis [6]. This analysis technique allows studying different parameters, such as the amplitudes of rainfall, frequency, and phase angle (showing time of maximum rainfall). Harmonic analysis technique has been used by many researchers to investigate

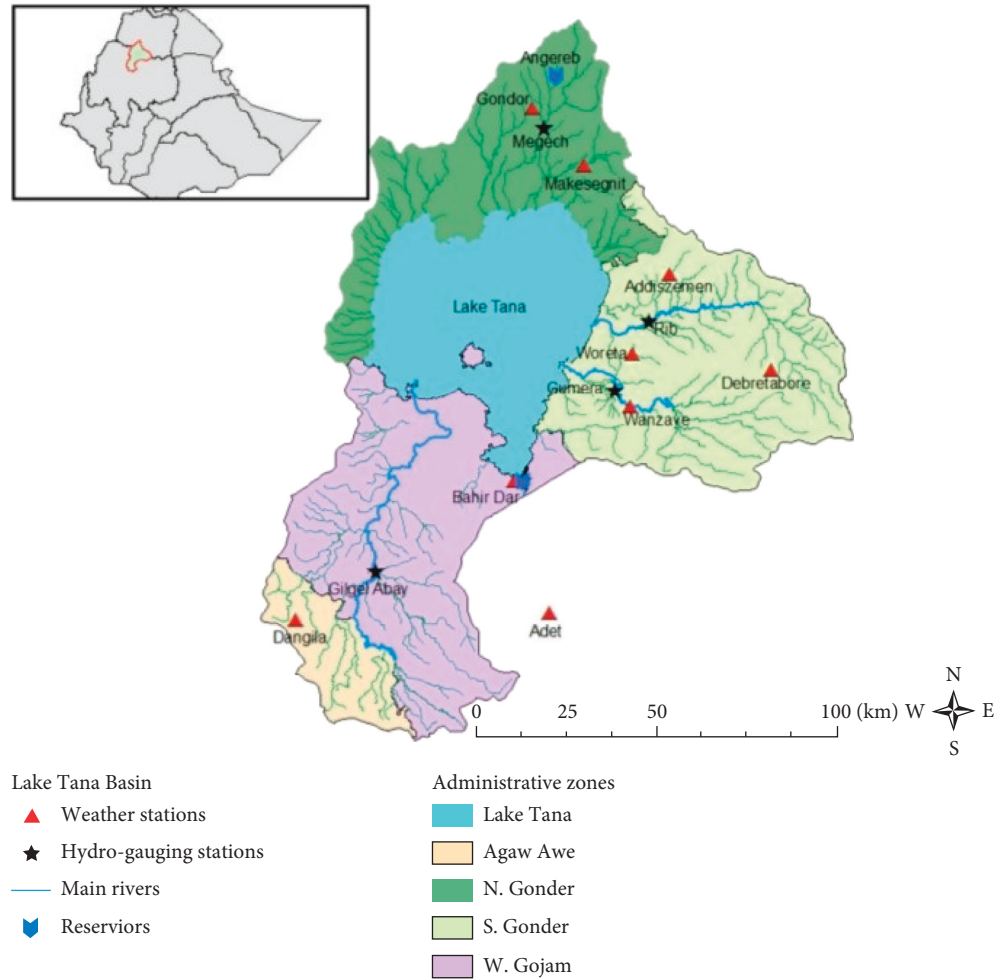


FIGURE 1: The location of the Lake Tana Basin in the Ethiopian and the Upper Blue Nile Basin system with meteorological stations ([16]).

the spatial and temporal distribution of rainfall. Hsu and Wallace [7] have investigated seasonal precipitation in global scale using harmonic analysis and found much less seasonal variation of precipitation over the oceans than the land. Horn and Bryson [8] and McGee [9] also studied the seasonal distribution and climatology of precipitation using harmonic analysis. Tarawneh [10] presented rainfall climatology of Saudi Arabia. Tarawneh and Kadioglu [11] and Kadioglu et al. [12] used the harmonic technique to analyze precipitation climatology in Jordan and Turkey, respectively; the results of these two articles agree with each other in terms of the percentages of variance of the first harmonic, which represent more than 90% of variation. This is due to the fact that Jordan and Turkey are located in the Mediterranean region and are affected by similar weather systems. The above studies have demonstrated the efficiency of the harmonic analysis technique in analyzing precipitation time series in terms of the amplitudes of many harmonics and periodicity.

Variability and distribution of precipitation within the Upper Blue Nile Basin, where the Lake Tana Basin is found (Figure 1), has been investigated by many researchers (e.g., [13, 14]). Similarly, Worku [15] stated that flooding is a familiar event in the Upper Blue Nile Basin and did cause

a lot of destruction in the past years. But those all researchers did not explain the features of precipitation in terms of percentage of variance, amplitude, and phase shift since the actual data they used cannot show the hidden features of precipitation distribution at different harmonics. Even though harmonic analysis gives us better understanding of the periodicity of annual, seasonal, and interseasonal rainfall, none of these studies have applied this method in the region. Therefore, this study aims to investigate the seasonal and annual cycles of rainfall in the Lake Tana Basin using harmonic analysis. We have utilized 31-year precipitation data gathered at four separate meteorological stations within the Lake Tana Basin.

### 1.1. Synoptic Climatology of Rainfall in Lake Tana Basin.

The climate of Lake Tana Basin is dominated by highland tropical monsoon, seasonal migration of intertropical convergence zone (ITCZ), and associated atmospheric circulations, but the complex topography of the region has also an effect on local climate conditions. Even if the basin is found within the tropics, it is not a hot region since the altitudinal climate controlling effect is significantly higher than its latitudinal controlling effect. In other words, Lake

TABLE 1: Stations of the studying area, locations, elevations, and mean annual rainfall.

| Station name | Latitude (degree) | Longitude (degree) | Elevation (m) | Mean annual rainfall (mm) |
|--------------|-------------------|--------------------|---------------|---------------------------|
| Bahir Dar    | 11.57             | 37.36              | 1800          | 1403.17                   |
| Debre Tabor  | 11.86             | 38.02              | 2706          | 1459.40                   |
| Gondar       | 12.60             | 37.45              | 1967          | 1069.40                   |
| Dangila      | 11.25             | 36.84              | 2127          | 1633.10                   |

Tana Basin, because of its high altitudes, mostly experiences temperate climate conditions. Thus, the seasonal variation in the climate is low compared to other tropical areas of low altitude [17].

Two distinct seasons, dry and wet, are documented. The dry season is from November to May, while the wet season covers the remaining parts of the year, when most of the precipitation takes place. Summer season from June to September is the most important and agriculturally active season, most of the rainfall (70–90% total rainfall) occurs, in the basin. The mean annual rainfall of the area is about 1465 mm with significant spatial variation. The mean annual maximum temperature is 25.5°C, and the mean annual minimum temperature is 10.8°C [18].

## 2. Methodology

**2.1. The Study Area.** The Lake Tana (shown in Figure 1) is located in Northwestern Ethiopia (latitude 10.95° and 12.78°N and longitude 36.89° and 38.25°E) with a drainage area of about 15,000 km<sup>2</sup> [19]. The Lake Tana Basin (Figure 1), the largest lake in Ethiopia and the third largest in the Nile Basin, is found in this region. It is shared by three administrative zones of the Amhara regional state, namely, North Gondor, South Gondor, and West Gojjam directly. The climate of the area is largely controlled by the movement of the intertropical convergence zone and tropical highland monsoon, which results in a single rainy season between June and September. 70–90% of total rainfall occurs in kiremt season between June and September. The mean annual rainfall varies from 1,200 to 1,600 mm [20], and the mean actual evapotranspiration of the catchments is 773 mm.

**2.2. Data.** The main data used in this study are monthly precipitation for each year in the whole statistical period, which are collected from the National Meteorology Agency (NMA) of Ethiopia. We have used four weather stations (Table 1) which spread out over the Lake Tana Basin along with a full statistical period of 31 years (1985–2015). Station selection was based on quality, long range data, and representation of various climate zones in the Basin. Some station selection criteria justify that the study of historical climate variability and change should utilize reliable data that are free of artificial trends or changes. Artifacts of measurement caused by changes in observation practice, equipment, site exposure, and location can lead to misleading results when used in trend analyses [21]. Hence, the homogeneity test of the time series of precipitation data, following reliable procedures (e.g., [22]), have been applied

in this study to reduce these artifacts. We have used the total monthly average precipitation for the harmonic analysis.

**2.3. Harmonic Analysis.** Harmonic analysis is commonly used to study periodic variations that can represent the fluctuations or variations in a time series as having arisen from adding together a series of sine and cosine functions [6, 23]. It is based on the mathematical principle that a curve, viewed as a function, may be represented by a series of trigonometric function. These trigonometric functions are “harmonic” in the sense that they are chosen to have frequencies exhibiting integer multiples of the fundamental frequency determined by the sample size (i.e., length) of the data series [24].

**2.3.1. Representation of Seasonal and Annual Cycles by Transforming a Cosine Wave.** Necessarily, harmonic function laterally shifts in order to have it match the peaks and troughs of a data series. The time series data represented by  $Y$ ,  $t = 0$ , at origin  $Y$ , can be written as a combination of different sine and cosine signals as follows:

$$Y = \bar{y} + A_1 \cos\left(\frac{2\pi t}{T} - \Phi_1\right) + A_2 \cos\left(\frac{4\pi t}{T} - \Phi_2\right) + \dots + A_n \cos\left(\frac{2n\pi t}{T} - \Phi_n\right), \quad (1)$$

where  $\bar{y}$  is an arithmetic average of the original data series, while the rest of the terms represent the first, second, ...,  $n$ th harmonics of the period  $T$  and  $\Phi$  is called the phase angle or phase shift which can then be easily interpreted as corresponding to the time of maximum harmonic function.

This time shifting is most conveniently accomplished when the cosine function is used because its maximum value is achieved when the angle on which it operates is zero. Shifting the cosine function to the right by the angle  $\Phi$  results in a new function that is maximized at  $\Phi$ .

Equation (1) can be rewritten as a series:

$$Y = \bar{y} + C \cos\left(\frac{2\pi t}{T} - \Phi\right). \quad (2)$$

The argument of cosine function is zero when

$$\Phi = \frac{2\pi t}{T}. \quad (3)$$

The function is maximized at time

$$t_i = \frac{\Phi_i T}{2\pi}, \quad (4)$$

where  $t_i$  is the  $i$ th month and  $\Phi_i$  is the phase shift for the corresponding month of the data series.

**2.3.2. Estimation of the Harmonic Parameters.** In order to calculate amplitude ( $C$ ) and phase shift ( $\Phi$ ) of a periodicity for which the data comprise a perfect sine curve for a known period  $T$ , direct substitution is being applied. For representing the associated precipitation data reasonably well, better choices for  $C$  and  $\Phi$  can be found [6, 23]. The easiest way to do this is by applying trigonometric identity approach.

$$\cos(\alpha - \Phi) = \cos \Phi \cos \alpha + \sin \alpha \sin \Phi. \quad (5)$$

For  $\alpha = 2\pi t/T$  and multiplying both sides by amplitude  $C$  reveals the following equation:

$$\begin{aligned} C \cos\left(\frac{2\pi t}{T} - \Phi\right) &= C \cos \Phi \cos\left(\frac{2\pi t}{T}\right) + C \sin \Phi \sin\left(\frac{2\pi t}{T}\right) \\ &+ A \cos\left(\frac{2\pi t}{T}\right) + B \sin\left(\frac{2\pi t}{T}\right), \end{aligned} \quad (6)$$

where  $A = C \cos \Phi$  and  $B = C \sin \Phi$ .

$$Y = \hat{y} + A \cos\left(\frac{2\pi t}{T}\right) + B \sin\left(\frac{2\pi t}{T}\right), \quad (7)$$

where

$$C = [A^2 + B^2]^{1/2}. \quad (8)$$

For  $n$ th order of harmonics, (6) can be rewritten as follows:

$$Y = \hat{y} + \sum_{i=1}^n \left[ a_i \cos\left(\frac{2\pi t_i}{T}\right) + b_i \sin\left(\frac{2\pi t_i}{T}\right) \right]. \quad (9)$$

Similarly,

$$A_i = [a_i^2 + b_i^2]^{1/2}, \quad (10)$$

$$\Phi_i = \tan^{-1}\left(\frac{b_i}{a_i}\right). \quad (11)$$

For the special situation where the data values are equally spaced in time with no missing values, the properties of the sine and cosine functions allow the same least-squares parameter values to be obtained more easily and efficiently using the following equation:

$$\begin{aligned} a_i &= \frac{2}{N} \sum_{t=1}^{N-1} Y \cos\left(\frac{2\pi t_i}{T}\right), \\ b_i &= \frac{2}{N} \sum_{t=1}^{N-1} Y \sin\left(\frac{2\pi t_i}{T}\right), \end{aligned} \quad (12)$$

where  $i = 1, 2, 3, \dots, N/2$ ,  $a_i$  and  $b_i$  are coefficients of the  $i$ th harmonic given by [6, 25], and  $Y$  is the monthly mean precipitation of the  $i$ th month, and  $N$  is the number of observations.

The variance of harmonic can be also obtained using Wilks [6]:

$$V_i = \frac{A_i^2}{2}. \quad (13)$$

The percentage of the total month-to-month variations explained by a given harmonic can be determined by forming a ratio of the square of the amplitude of that specific harmonic to the sum of all harmonics. The first harmonic can show the observed data of precipitation as a single annual cycle, whereas the second harmonic can represent the tendency towards a semiannual variation of precipitation that cannot be observed from the observed data [10]. With the same concept, the third harmonic describes more detail of the annual variation of precipitation and so on. In brief, the first harmonics show an annual cycle with the greatest amplitude as compared to other harmonics. The second harmonic indicates a semiannual change, while the third one illustrates four-month seasonal change in details [12]. The phase angle shift indicates the displacements of the maximum along the time axis, which can be represented by the  $x$ -axis. The phase angle shift can express the precipitation regime and the boundaries [26].

### 3. Result and Discussion

In order to obtain the dominant harmonics, we have calculated different parameters. Consequently, Table 2 shows the calculations necessary to obtain least-square estimates for the parameters of the annual harmonic representing the Lake Tana Basin's mean monthly precipitation, using (12). The precipitation data are shown in the column labeled  $Y$  in Table 2.

Figure 2 illustrates the foregoing procedure using the mean monthly precipitation (mm) for 1985–2015 in the Lake Tana Basin. This figure is simply a plot of the 12 data points, with  $t = 1$  indicating January,  $t = 2$  indicating February, and so on. The monthly annual average precipitations, which are represented by dotted points, are 122.06, 116.93, 89.11, and 136.08 mm for Debre Tabor, Bahir Dar, Gondar, and Dangila, respectively. The lowest value of precipitation over Gondar station is due to the surrounding areas' dryness which implies that the wind flow from the dry land does not bring enough amount of moisture. The consecutive occurrence of wet and dry sequences can alter the variability of precipitation distribution which depends on regional-scale predictors such as humidity and atmospheric pressure as Wilby et al. [27] found. In addition to this, we suppose that, land cover of the area will also be the possible reason, but it needs farther study. So, the rainfall of Gondar has been (highly) variable in time and concentrated in summer season (at  $t = 7$  (July) and  $t = 8$  (August), Figure 2), considering the above point. Other studies also conclude that the rainfall of mountainous areas is highly variable from time to time and from station to station [28, 29]. Those all bring high interannual and semiannual variability of precipitation as the percentage of variation as shown in Figure 4.

TABLE 2: Illustration of the mechanics of using (2), (3), and (5)–(13) to estimate the parameters of a fundamental harmonic for each station.

| <i>(a) Debre Tabor</i> |         |                   |                   |                     |                     |        |
|------------------------|---------|-------------------|-------------------|---------------------|---------------------|--------|
| Serial number          | Y       | $\cos(2\pi t/12)$ | $\sin(2\pi t/12)$ | Y $\cos(2\pi t/12)$ | Y $\sin(2\pi t/12)$ |        |
| 1                      | 406.88  | -0.5000           | -0.8660           | -203.44             | -352.36             |        |
| 2                      | 389.11  | -0.8660           | -0.5000           | -336.97             | -194.56             |        |
| 3                      | 183.86  | -0.0000           | -1.0000           | 0.00                | -183.86             |        |
| 4                      | 165.34  | -1.0000           | 0.0000            | -165.34             | 0.00                |        |
| 5                      | 76.86   | 0.5000            | -0.8660           | 38.43               | -66.56              |        |
| Sum                    | 1222.05 | -1.866            | -3.232            | -667.32             | -798.34             |        |
|                        | $a_i$   | $b_i$             | $A_i$             | $\Phi_i$ (rad)      | $V_i$               | $PV_i$ |
| 1                      | -33.91  | -58.56            | 67.67             | 1.05                | 2289.6              | 4.47   |
| 2                      | -90.07  | -90.99            | 128.03            | 0.79                | 8195.9              | 15.99  |
| 3                      | -90.07  | -121.63           | 151.35            | 0.93                | 11,453.2            | 22.35  |
| 4                      | -117.63 | -121.63           | 169.21            | 0.80                | 14,315.3            | 27.93  |
| 5                      | -111.22 | -132.72           | 173.16            | 0.87                | 14,992.2            | 29.26  |
| <i>(b) Bahir Dar</i>   |         |                   |                   |                     |                     |        |
| Serial number          | Y       | $\cos(2\pi t/12)$ | $\sin(2\pi t/12)$ | Y $\cos(2\pi t/12)$ | Y $\sin(2\pi t/12)$ |        |
| 1                      | 417.04  | -0.867            | -0.498            | -361.57             | -207.69             |        |
| 2                      | 381.08  | -0.502            | -0.865            | -191.30             | -329.63             |        |
| 3                      | 195.84  | -0.000            | -1.000            | 0.00                | -195.84             |        |
| 4                      | 184.91  | -1.000            | 0.000             | -184.91             | 0.00                |        |
| 5                      | 92.16   | 0.498             | -0.867            | 45.90               | -79.90              |        |
| Sum                    | 1271.39 | -1.871            | -3.23             | -691.88             | -813.06             |        |
|                        | $a_i$   | $b_i$             | $A_i$             | $\Phi_i$ (rad)      | $V_i$               | $PV_i$ |
| 1                      | -60.26  | -34.62            | 69.50             | 0.52                | 2414.91             | 4.55   |
| 2                      | -91.14  | -89.56            | 127.78            | 0.78                | 8163.75             | 15.38  |
| 3                      | -91.14  | -122.20           | 154.26            | 0.93                | 11897.59            | 22.41  |
| 4                      | -121.95 | -122.20           | 172.64            | 0.79                | 14902.32            | 28.07  |
| 5                      | -114.30 | -135.52           | 177.29            | 0.87                | 15715.08            | 29.60  |
| <i>(c) Gondar</i>      |         |                   |                   |                     |                     |        |
| Serial number          | Y       | $\cos(2\pi t/12)$ | $\sin(2\pi t/12)$ | Y $\cos(2\pi t/12)$ | Y $\sin(2\pi t/12)$ |        |
| 1                      | 288.34  | -0.8660           | -0.5000           | -249.70             | -144.17             |        |
| 2                      | 282.9   | -0.5000           | -0.8660           | -141.45             | -244.99             |        |
| 3                      | 154.35  | -1                | 0.00              | -154.35             | 0.00                |        |
| 4                      | 107.51  | -0.00             | -1                | 0.00                | -107.51             |        |
| 5                      | 82.02   | -0.8660           | 0.5000            | -71.03              | 41.01               |        |
| Sum                    | 915.12  | -3.232            | -1.866            | -616.53             | -455.66             |        |
|                        | $a_i$   | $b_i$             | $A_i$             | $\Phi_i$ (rad)      | $V_i$               | $PV_i$ |
| 1                      | -41.62  | -24.03            | 48.06             | 0.17                | 1154.83             | 4.22   |
| 2                      | -65.20  | -64.86            | 91.97             | 0.78                | 4228.93             | 15.46  |
| 3                      | -90.93  | -64.86            | 111.69            | 0.62                | 6237.54             | 22.81  |
| 4                      | -90.93  | -82.78            | 122.97            | 0.74                | 7560.40             | 27.65  |
| 5                      | -102.77 | -75.94            | 127.78            | 0.64                | 8164.28             | 29.86  |
| <i>(d) Dangila</i>     |         |                   |                   |                     |                     |        |
| Serial number          | Y       | $\cos(2\pi t/12)$ | $\sin(2\pi t/12)$ | Y $\cos(2\pi t/12)$ | Y $\sin(2\pi t/12)$ |        |
| 1                      | 382.32  | -0.5000           | -0.8660           | -191.16             | -331.09             |        |
| 2                      | 362.28  | -0.8660           | -0.5000           | -313.73             | -181.14             |        |
| 3                      | 261.57  | -1                | 0.00              | -261.57             | 0.00                |        |
| 4                      | 254.58  | 0.00              | -1                | 0.00                | -254.58             |        |
| 5                      | 150.99  | -0.8660           | 0.5000            | -130.76             | 75.50               |        |
| Sum                    | 1411.74 | -3.232            | -1.866            | -897.22             | -691.31             |        |
|                        | $a_i$   | $b_i$             | $A_i$             | $\Phi_i$ (rad)      | $V_i$               | $PV_i$ |
| 1                      | -31.86  | -55.18            | 63.72             | 1.05                | 2029.95             | 3.68   |
| 2                      | -84.15  | -85.37            | 119.87            | 0.79                | 7184.63             | 13.03  |
| 3                      | -127.75 | -85.37            | 153.65            | 0.59                | 11,804.05           | 21.40  |
| 4                      | -127.75 | -127.80           | 180.70            | 0.79                | 16,326.45           | 29.60  |
| 5                      | -149.46 | -115.22           | 188.72            | 0.66                | 17,806.97           | 32.29  |

The monthly maximum precipitation values are 406.88 (August), 417.04 (July), 288.34 (July), and 382.32 (August) for Debre Tabor, Bahir Dar, Gondar, and Dangila, respectively. These data appear to be at least approximately

sinusoidal, executing a single full-cycle over the course of the 12 months. The precipitation at Bahir Dar station shows the annual peak of 417.04 mm in July and the annual valley value of 1.66 mm in January (Figure 2 for all the other

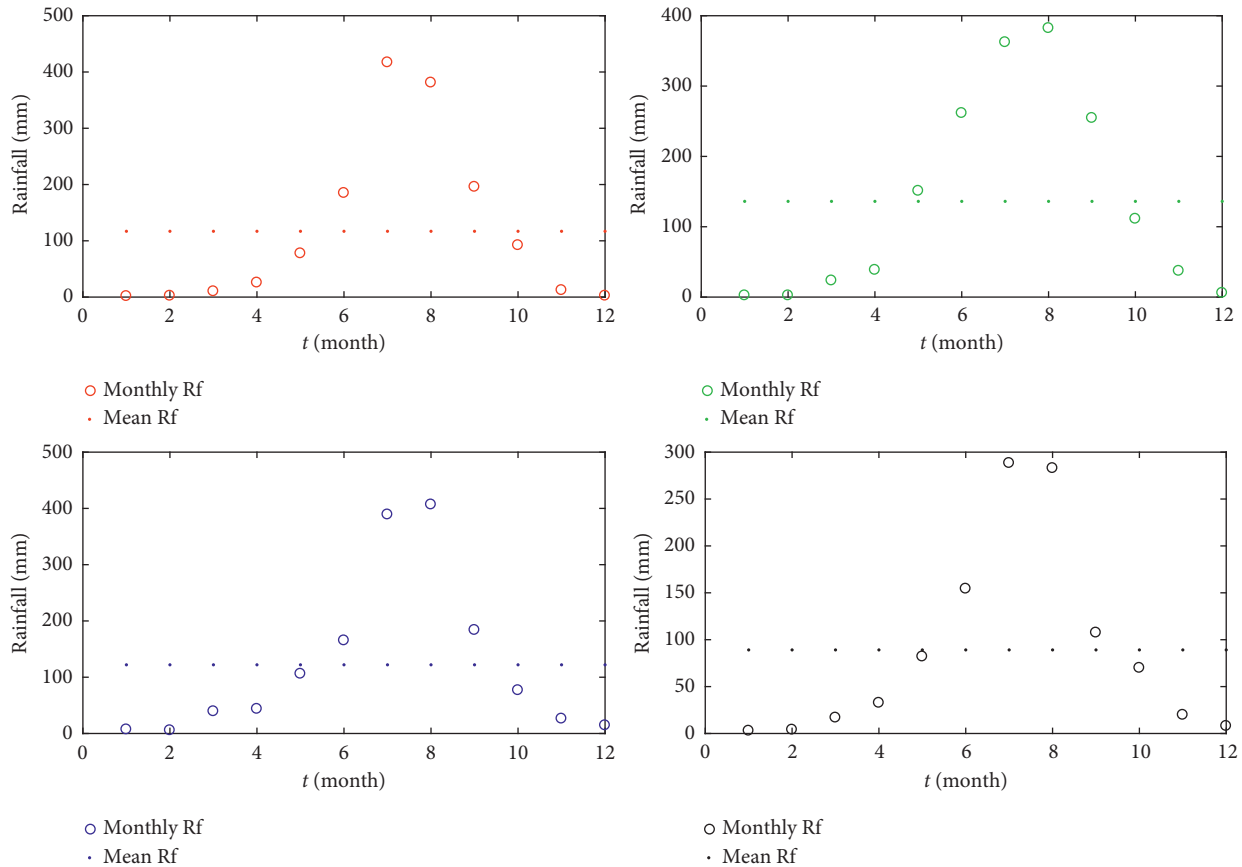


FIGURE 2: The monthly precipitation (mm) averaged over 1985–2015 for the four stations: (a) Bahir Dar, (b) Dangila, (c) Debre Tabor, and (d) Gondar. Circular points show climatic mean, and horizontal dotted lines show annual mean.

stations). Generally, the annual maximum precipitation for all stations occurred in July and August which are the months of main rainy season for the region and most parts of Ethiopia [20].

The blue curve at Figure 3 shows the function lifted to the level of the average annual precipitation and stretched so that its range is similar to that of the data series (2), with  $\phi = 0$ . The stretching has been done only approximately, by choosing the amplitude  $C$  to be the maximum precipitation value between the January and December. Simply it is a cosine function with the argument transformed so that it executes one full cycle in 12 months. It is obviously a poor representation of the data because the representation of the curve is opposite to the normal data distribution which is represented by the circular points. Hence, the cosine curve needs to be shifted downward to line up well with the data. The five harmonics plotted downward are used to overcome this poor representation of the data. The maximum in the curve can be made to occur at  $t = 7$  months (July) and  $t = 8$  months (August) by introducing the phase shift, using (3), of  $\phi = 7(2\pi/12) = (7/6)\pi$  and  $\phi = 8(2\pi/12) = (4/3)\pi$ .

From Figure 3, we can also see that the first five harmonics represent the data distribution appropriately. Accordingly, the first two harmonics green (1st) and red (2nd) curves show the dominant harmonics which occur in July

(for Bahir Dar and Gondar) and August (for Debre Tabor and Dangila), respectively. The amplitudes for the first harmonic are 173.42, 177.93, 127.77, and 188.78 mm for Debre Tabor, Bahir Dar, Gondar, and Dangila, respectively.

Figure 4 shows the percentage of variance for each harmonic. The percentages of variance for the first harmonics are 3.68, 4.22, 4.48, and 4.55 in Dangila, Gondar, Debre Tabor, and Bahir Dar, respectively, which represents low variations that can assure that there is difference in climatic regime in the basin. The percentages of variance for the second harmonic are 13.03, 15.38, 15.46, and 15.99 in Dangila, Bahir Dar, Gondar, and Debre Tabor, respectively. Similarly, the percentage of variance for third harmonic are 21.40, 22.35, 22.41, and 22.81 in Dangila, Debre Tabor, Bahir Dar, and Gondar, respectively, which exactly agrees with the definitions of percentage of variance; low percentage of variance for first harmonic necessarily increase the percentage of other harmonics [6, 10]. From the percentage of variance, the second and third harmonics have higher percentage than the first harmonic (Table 2 and Figure 4) which demonstrates that different parts of the basin do have different rainfall regimes.

As it is mentioned in the above, low percentages of the first harmonic variance require more contribution from high percentages of other harmonics (like semiannual or seasonal variations). The last harmonics indicates poor representation of the time series data.

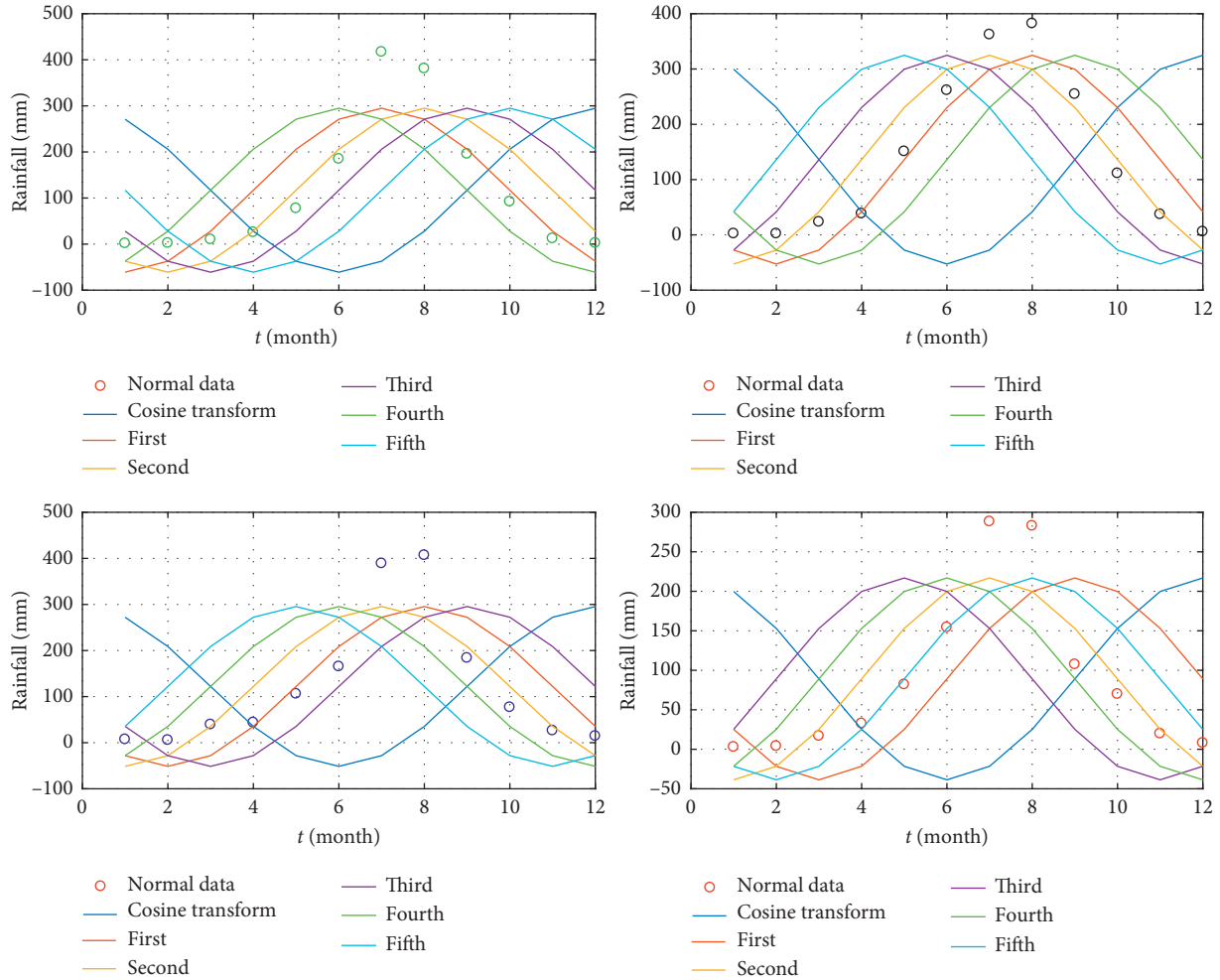


FIGURE 3: Illustration of the approximate matching of a cosine function to a data detail about the lines. (a) Bahir Dar, (b) Dangila, (c) Debre Tabor, and (d) Gondar.

### 4. Conclusion

We have presented the rainfall climatology of Lake Tana Basin using the harmonic analysis technique. This method is commonly used to study periodic variations that can represent the fluctuations or variations in a time series for diverse topographical features as having arisen from adding together a series of sine and cosine functions. Precipitation features are explained in terms of percentage of variances, amplitudes, and phase angle.

Climatologically, these regions are affected by various well-known weather conditions, such as ITCZ, ENSO, and so on, which affect different regions at specific times of the year. The percentages of variations are related to the effect of these conditions that usually affect each region separately. The maximum precipitation for all stations occurred in July and August. The annual average precipitation of Dangila was 136.08 mm which was the highest record than the other stations, and the average maximum monthly precipitation (417.04 mm) was recorded in Bahir Dar during July. The amplitudes for the first harmonic are 173.42, 177.93, 127.77, and 188.78 mm for Debre Tabor, Bahir Dar, Gondar, and Dangila, respectively. The percentage of variance shows lower

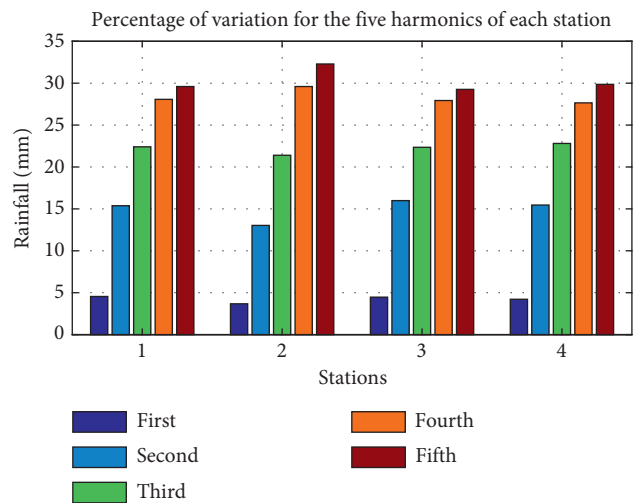


FIGURE 4: Percentage of variance for all stations (x-axis: 1 = Bahir Dar, 2 = Dangila, 3 = Debre Tabor, and 4 = Gondar).

value in the first harmonic than others, implying that there is difference in the climatic regime in the Lake Tana Basin. Low percentages of the first harmonic variance mean that it requires

more contribution from high percentages of other harmonics (like semiannual or seasonal variations).

In all stations, the original time series precipitation has been represented fairly by the first five harmonics. But the number of stations used in this study is less in number to represent the whole basin. Hence, we recommend extension of the number of stations and spatial coverage to incorporate the Upper Blue Nile Basin and beyond, performing the proposed data quality analysis and calculation of the harmonic parameters for further studies.

## Conflicts of Interest

The authors declare that there are no actual or potential conflicts of interest in relation to this article.

## Acknowledgments

The authors greatly acknowledge Bahir Dar University for their encouragement, the National Meteorology Agency of Ethiopia for providing meteorological station data, and Debre Tabor University for their financial support and encouragement.

## References

- [1] IPCC, *Climate Change 2007: Climate Change Impacts, Adaptation and Vulnerability*, Cambridge University Press, Cambridge, UK, 2007.
- [2] WMO, *Drought Monitoring and Early Warning Concept, Progress and Future*, World Meteorological Organization, Geneva, Switzerland, 2006.
- [3] M. Domroes and D. Schaefer, "Recent climate change affecting rain- storm occurrences, a case study in East China," *Climate of the Past Discussions*, vol. 4, no. 2, pp. 289–308, 2008.
- [4] J. Huang, S. Sun, Y. Xue, and J. Zhang, "Changing characteristics of precipitation during 1960–2012 in inner Mongolia, northern China," *Meteorology and Atmospheric Physics*, vol. 127, no. 3, pp. 257–271, 2015.
- [5] M. Kawser Ahmed, M. Samsul Alam, A. H. Muhammad Yousuf, and M. Monirul Islam, "A long-term trend in precipitation of different spatial regions of Bangladesh and its teleconnections with El Niño/Southern oscillation and Indian Ocean Dipole," *Theoretical and Applied Climatology*, vol. 129, no. 1-2, pp. 473–486, 2016.
- [6] D. S. Wilks, *Statistical Methods in the atmospheric Sciences: An Introduction*, Academic Press, San Diego, CA, USA, 2006.
- [7] C. P. F. Hsu and J. M. Wallace, "The global distribution of the annual and semiannual cycles in precipitation," *Monthly Weather Review*, vol. 104, no. 9, pp. 1093–1101, 1976.
- [8] L. H. Horn and R. A. Bryson, "Harmonic analysis of the annual march of precipitation over the United States," *Annals of the Association of American Geographers*, vol. 50, no. 2, pp. 157–171, 1960.
- [9] O. S. McGee, "The use of the harmonic dial in rainfall climatology," *South African Geographical Journal*, vol. 51, no. 1, pp. 65–72, 1969.
- [10] Q. Tarawneh, "Harmonic analysis of precipitation climatology in Saudi Arabia," *Theoretical and Applied Climatology*, vol. 124, no. 1-2, pp. 205–217, 2015.
- [11] Q. Tarawneh and M. Kadioglu, "An analysis of precipitation climatology in Jordan," *Theoretical and Applied Climatology*, vol. 74, no. 1-2, pp. 123–136, 2002.
- [12] M. Kadioglu, N. Ozturk, H. Erdun, and Z. Sen, "On the precipitation climatology on Turkey by harmonic analysis," *International Journal of Climatology*, vol. 19, no. 15, pp. 1717–1728, 1999.
- [13] M. Osman and P. Sauerborn, "A preliminary assessment of characteristics and long-term variability of rainfall in Ethiopia—basis for sustainable land use and resource management," in *Proceedings of the Conference on International Agricultural Research for Development*, Kassel-Witzenhausen, Germany, Deutscher Tropentag, 2002.
- [14] Z. Segele and P. Lamb, "Characterization and variability of Kiremt rainy season over Ethiopia," *Meteorology and Atmospheric Physics*, vol. 89, no. 1-4, pp. 153–180, 2005.
- [15] L. Y. Worku, "Climate change impact on variability of rainfall intensity in the Upper Blue Nile Basin," *Proceedings of the International Association of Hydrological Sciences*, vol. 366, pp. 135–136, 2015.
- [16] Y. T. Dile, R. Berndtsson, and S. G. Setegn, "Hydrological Response to Climate Change for Gilgel Abay River, in the Lake Tana Basin-upper Blue Nile Basin of Ethiopia," *PLoS One*, vol. 8, no. 10, article e79296, 2013.
- [17] S. A. Legese, O. A. Olutayo, H. Sulaiman, and P. Rao, "Assessing climate change impacts in the Lake Tana Sub-Basin, Ethiopia using livelihood vulnerability approach," *Journal of Earth Science & Climatic Change*, vol. 7, p. 368, 2016.
- [18] S. L. Gebre and F. Ludwig, "Hydrological response to climate change of the upper blue Nile River Basin: based on IPCC fifth assessment report (AR5)," *Journal of Climatology & Weather Forecasting*, vol. 3, p. 121, 2015.
- [19] MoWR, *Abay River Basin Integrated Development Master Plan Project: 140*, Ministry of Water Resources, River Development & Ganga Rejuvenation, New Delhi, India, 1998.
- [20] S. G. Setegn, R. Srinivasan, A. M. Melesse, and B. Dargahi, "SWAT model application and prediction uncertainty analysis in the Lake Tana Basin, Ethiopia," *Hydrological Processes*, vol. 24, no. 3, pp. 357–367, 2010.
- [21] T. R. Karl, P. D. Jones, R. W. Knight et al., "Asymmetric trends of daily maximum and minimum temperature," *Bulletin of the American Meteorological Society*, vol. 74, no. 6, pp. 1007–1023, 1993.
- [22] T. Szentimrey, *Report with Final Results of the Data Harmonization Procedures Applied Including All Protocols, Per Country*, OJEU 2010/S 110-166082, 1999.
- [23] K. I. Kirkyla and S. Hameed, "Harmonic analysis of the seasonal cycle in precipitation over the United States: a comparison between observation and a general circulation model, American Meteorological Society," *Journal of Climate*, vol. 2, no. 12, pp. 1463–1475, 1989.
- [24] M. Moghbel, M. Davoudi, A. Neyestani, and F. Taghavi, "Spatial and temporal study of precipitation characteristics over Iran," *Geography and Environmental Planning Journal*, vol. 51, no. 3, pp. 29–32, 2013.
- [25] H. A. Panofsky and G. W. Brier, *Some Applications of Statistics to Meteorology*, Pennsylvania State University, State College, PA, USA, 1958.
- [26] J. C. Davis, *Statistical and Data Analysis in Geology*, John Wiley, New York, NY, USA, 1986.
- [27] R. L. Wilby, S. P. Charles, E. Zorita, B. Timbal, P. Whetton, and L. O. Mearns, "Guidelines for use of climate scenarios developed from statistical downscaling methods," in *Proceedings of the IPCC Task Group on Data and Scenario Support*

*for Impacts and Climate Analysis (TGICA 2004)*, Laxenburg, Austria, September 2004.

- [28] E. Mersha, "Assessment of moisture availability over semi-arid and arid zones of Ethiopia," *Ethiopian Journal of Natural Resources*, vol. 5, pp. 165–191, 2003.
- [29] W. Bewket and D. Conway, "A note on the temporal and spatial variability of rainfall in the drought-prone Amhara region of Ethiopia," *International Journal of Climatology*, vol. 27, pp. 1467–1477, 2007.



**Hindawi**

Submit your manuscripts at  
[www.hindawi.com](http://www.hindawi.com)

